BMC Biotechnology

RESEARCH

Open Access

Enhancement of plasma kallikrein specificity of antitrypsin variants identified by phage display and partial reversion

Sangavi Sivananthan[1], Tyler Seto[1], Negin C. Tehrani[1], Varsha Bhakta[1,2] and William P. Sheffield[1,2*]

Abstract

Background The naturally occurring variant Alpha-1 Antitrypsin M358R (AAT M358R), modified at the P1 position of the reactive center loop (RCL), shifts its inhibitory protease target from neutrophil elastase to multiple coagulation and contact proteases, including activated plasma kallikrein (Pka; KLKB1). Our aim was to increase the specificity of AAT M358R for Pka as a potential novel therapeutic agent to treat pathological swelling arising from elevated Pka levels in patients with Hereditary Angioedema.

Results Two AAT M358R T7Select phage display libraries randomized at RCL positions P7-P3 and P2-P3′ were iteratively probed with Pka. The most abundant Pka-inhibitory motifs from phage display were P7-P3, **Q**L**IPS**; and P2-P3′, **V**R**RAY** (mutated residues in bold). AAT variants expressing these motifs, alone or in combination, as well as six less-mutated P7-P3 revertant proteins were expressed, purified, and characterized kinetically. Variants AAT M358R (QLIPS) (designated 7-QLIPS-3) and 7-FLEPS-3 exhibited significantly enhanced selectivity for Pka (over factor XIa) by factors of 6.9 and 9.2, respectively, without increasing the stoichiometry of inhibition (SI) or decreasing the inhibition rate relative to AAT M358R. No other variants matched this profile.

Conclusions Pro substitution at P4 was found to be important for enhanced inhibition of Pka by AAT M358R. Two novel variants with this substitution are more rapid and selective inhibitors of Pka than AAT M358R and may provide better control of Pka in vivo than existing HAE therapeutics.

Keywords Phage display, Alpha-1 antitrypsin, Plasma kallikrein, Mutagenesis, Reactive centre loop, Hereditary angioedema

*Correspondence:
William P. Sheffield
sheffiel@mcmaster.ca
[1]Department of Pathology and Molecular Medicine HSC 4H19, McMaster University, 1280 Main Street West, Hamilton, ON L8S 4K1, Canada
[2]Canadian Blood Services, Innovation and Portfolio Management, Medical Affairs and Innovation, Hamilton, ON, Canada

© The Author(s) 2025. **Open Access** This article is licensed under a Creative Commons Attribution-NonCommercial-NoDerivatives 4.0 International License, which permits any non-commercial use, sharing, distribution and reproduction in any medium or format, as long as you give appropriate credit to the original author(s) and the source, provide a link to the Creative Commons licence, and indicate if you modified the licensed material. You do not have permission under this licence to share adapted material derived from this article or parts of it. The images or other third party material in this article are included in the article's Creative Commons licence, unless indicated otherwise in a credit line to the material. If material is not included in the article's Creative Commons licence and your intended use is not permitted by statutory regulation or exceeds the permitted use, you will need to obtain permission directly from the copyright holder. To view a copy of this licence, visit http://creativecommons.org/licenses/by-nc-nd/4.0/.

Introduction

Hereditary Angioedema (HAE) is an autosomal dominant disease marked by recurrent episodes of acute swelling affecting different body regions [12, 24, 49]. HAE is classified into three types: Type 1, arising from quantitative genetic deficiency of C1-esterase inhibitor (C1INH); Type 2, arising from quantitative genetic deficiency of functional C1INH; and the more rare Type 3, arising from genetic lesions in genes other than that encoding C1INH (C1INH) [7, 42, 54]. C1INH is a serpin that regulates complement, coagulation, and inflammatory pathways, by inhibiting various proteases, including activated plasma kallikrein (Pka) [15, 16, 22]. Pka catalyzes the cleavage of high molecular weight kininogen, liberating bradykinin, a key mediator of vasodilation and increased permeability during inflammation [25, 29, 38, 51]. Despite C1INH being recognized as the primary inhibitor of Pka, and replacement therapy with C1INH concentrates being the first specific therapy to show efficacy in ameliorating HAE [50], C1INH has limitations, due to its broad-spectrum inhibition of various proteases and its relatively slow rate of inhibition of Pka illustrated by a mean second order rate constant (k_2) of $\sim 2.55 \times 10^4$ $M^{-1}s^{-1}$ [21, 52]. While many pharmacological agents have been licensed for Pka control, some suffer from short half-lives [26, 27, 43] rendering them unsuitable for prophylactic administration, while other newer agents appropriate for prophylaxis are associated with high costs [1, 45, 48]. Opportunities remain, therefore, to develop new molecules for the optimal control of Pka in HAE, including engineered versions of other serpins.

The most abundant serpin in plasma, Alpha-1 Antitrypsin (AAT), exerts minimal influence on the contact system and primarily targets neutrophil elastase. However, a point mutation changing M358 to R358 (M358R), in the reactive center of AAT changes its specificity from inhibiting neutrophil elastase to inhibiting multiple coagulation/contact system proteases [18, 32, 37, 40, 47]. Inspired by this "experiment of nature", researchers have made additional modifications within the reactive center loop (RCL) of AAT M358R to enhance specificity toward coagulation and contact proteases [3, 8, 17, 33, 41]. One strategy for introducing and assessing RCL mutations involves creating serpin libraries with hypervariable RCL positions. Such a library can be functionally screened through phage display and biopanning, a method utilizing bait proteases in solution to probe variant proteins expressed on the T7 phage surface [9, 11].

Herein, two AAT M358R phage display libraries hypervariable between P7-P3′ were screened with Pka. Novel AAT M358R variants were expressed corresponding to the most abundant motifs, their combination, and their reversion towards AAT M358R. Our findings indicated that two novel mutated proteins demonstrated enhanced selectivity for Pka over activated factor XI (FXIa) without altering the rate of PKa inhibition or increasing the stoichiometry of inhibition (SI) relative to AAT M358R.

Methods

Materials

Purified human proteases Pka and FXIa were purchased from Enzyme Research Labs (South Bend, IN, USA). Chromogenic substrates (S-2302 for Pka and S-2366 for FXIa) were purchased from Diapharma (West Chester, OH, USA). Oligonucleotides were obtained from Integrated DNA Technologies (Coralville, IO, USA). Restriction endonucleases, thermostable DNA polymerase and buffers for PCR, gel extraction/purification kits, and glutathione agarose were obtained from ThermoFisher Scientific (Waltham, MA, USA). Nickel-nitrilotriacetic acid (Ni-NTA) agarose resin for nickel chelate affinity chromatography was obtained from Qiagen (Mississauga, Canada). PreScission protease, a fusion protein of glutathione sulfotransferase (GST)-human rhinovirus (HRV) 3 C protease, was acquired from ThermoFisher Scientific. Phage display libraries and plasmids pBAD-$H_6\alpha_1$PI M358R and pGEX-AAT M358R were generated previously by the Sheffield Laboratory [3].

DNA manipulation

Standard DNA manipulation techniques, including restriction digestion, electrophoresis, gel purification, ligation, and transformation of *E. coli*, were employed as previously described [3]. Cloning steps involved the use of *E. coli* DH5α, while *E. coli* BL21 was utilized for protein expression. All AAT M358R variant plasmids were verified by DNA sequencing at the Mobix Lab central facility, located in the Faculty of Health Sciences at McMaster University.

Biopanning of phage display libraries

T7Select10-3b API M358R(P7-P3ran) and T7Select10-3b API M358R(P2-P3′ ran) bacteriophage libraries were biopanned as previously described, with minor modifications [41]. Briefly, five rounds of biopanning with or without Pka were performed with each library, starting with 10^9 pfu/ml bacteriophage in liquid lysates. Phage populations reacting with Pka were captured using a biotinylated affinity-purified rabbit anti-human kallikrein IgG polyclonal antibody (Cusabio Technology, Houston, USA) and streptavidin-coated magnetic beads (Dynabeads, Invitrogen). The phage-antibody-bead assembly was used to infect *E. coli* BLT5403 cells to start subsequent rounds of biopanning.

To determine the phage titer in the lysate, a plaque assay was performed. *E. coli* BLT5403 was inoculated in Luria Broth (LB) with M9 salts (M9LB) and incubated at 37 °C until the OD_{600} reached 1.0. Phage lysate dilutions

(in LB) were separately plated on LB with ampicillin (LB-Amp) agar plates with *E. coli* BLT5403 M9LB growth culture (250 µl), a dilution of phage lysate (100 µl), and top agarose (4 ml). The plates were inverted, covered, and incubated overnight at room temperature for plaque counting.

Deep sequencing

Variant RCL sequences selected by AAT M358R phage display were determined using deep sequencing of polymerase chain reaction (PCR) products, as previously described [41]. Amplification of candidates was performed using phage lysates from: the starting library, the round 2 library selected with or without Pka, and the round 5 library selected with or without Pka. Sense oligonucleotides P504 and P505 were used, paired with antisense oligonucleotides P710, P711, and P712. The amplified products were analyzed on a 1.2% agarose gel, purified using a gel extraction kit (GeneJet Gel Extraction kit, ThermoFisher), and subjected to direct deep sequencing at McMaster University's Farncombe Metagenomics Facility, using an Illumina Nextra XT library kit. For sequence analysis, Linux operating software was used to convert FASTQ raw data files into FASTA format. The most abundant DNA and translated protein sequences in the phage lysate were identified using Clone Manager 7.11 software (Sci Ed Software, Westminster, Colorado, USA).

GST expression and purification

Expression vector pGEX-AAT M358R was created previously as described [3]. Each novel variant in this study was mobilized as a 1221 bp SalI-NcoI-ended minor fragment and ligated to the 4960 bp major fragment of pGEX-AAT M358R to create pGEX-AAT M358R(X) (where X is the motif of interest). *E. coli* BL21 transformed with pGEX-AAT M358R(X) variants were induced using 0.1mM isopropyl β-D-1-thiogalactopyranoside (IPTG), and purified using GST and nickel chelate (Ni-NTA) affinity chromatography purification methods, as previously described [3].

Protease inhibition assays with AAT M358R variants

The rate of inhibition of Pka or FXIa was quantified as the second order rate constant (k_2), which gives the rate as the product of the k_2 and the concentrations of protease and AAT M358R variants, as previously described, under pseudo first order conditions, by a discontinuous method [3]. The velocity of amidolysis of chromogenic substrates S-2302 (for Pka) and S-2366 (for FXIa) was evaluated at 37 °C in PPNE buffer (20m M sodium phosphate (pH 7.4), 0.1% (w/v) polyethylene glycol 8000, 100mM sodium chloride, and 0.1mM disodium ethylenediaminetetraacetic acid) using an Elx808 Absorbance Microplate Reader (Biotek, Winooski, VT, USA) at 405 nm. For k_2 determination, reactions included 10nM Pka/FXIa and 200nM AAT M358R variants, incubated for 8–30 s intervals and stopped with 100µM S-2302/S-2366 chromogenic substrate, respectively. Inhibition was also characterized by determination of the stoichiometry of inhibition (SI), which is an equilibrium measure of the number of inhibitor molecules required to inactivate one protease molecule [31]. For SI determination, reactions included 10nM Pka/FXIa and 10-1000nM AAT M358R variants, incubated for 2 h and stopped with 100µM S-2302/S-2366 chromogenic substrate. k_2 and SI were calculated as described previously [3].

Plasma clotting tests

The effects of AAT M358R or AAT M358R(X) proteins on in vitro clotting were assessed by measuring the diluted Activated Partial Thromboplastin Time, as previously described [3, 8]. Briefly, STA PTTA reagent (Diagnostica Stago, Asnières, France) was diluted 1:15 with Owren-Koller buffer (Diagnostica Stago). Normal human pooled plasma was supplemented with AAT M358R or variant protein to 3 µM final concentration, combined with diluted PTTA reagent, and pre-heated to 37°C. Citrate anticoagulation was overcome the addition of 50 µL of 25 mM $CaCl_2$, and clotting time was determined using a STA-IV clotting analyzer (Diagnostica Stago).

Electrophoretic analysis of AAT M358R variants with Pka/FXIa interactions

The electrophoretic profiles of the interaction between AAT M358R or AAT M358R(X) variants with Pka/FXIa were visualized on 10% (w/vol) sodium dodecyl sulfate (SDS)-polyacrylamide (SDS-PAGE) gels under reducing conditions. Reactions involved a final concentration of 2µM AAT M358R or AAT M358R(X) and 1µM Pka/0.2µM FXIa in PPNE buffer and were incubated at 37 °C for 1-5-minutes. Reactions were then terminated by adding 1/3 the reaction volume of concentrated 4x SDS-PAGE sample buffer and samples containing the entire reaction volume were subjected to electrophoresis. The gels were stained with Coomassie Brilliant Blue and destained as described previously [17]. Gels were imaged by using a model XR GelDoc system (Bio-Rad Laboratories, Mississauga, ON, Canada), and immunoblots were imaged by using a model Azure 280 system (Azure Biosystems, CA, USA).

Protein modeling

The Michaelis complexes between AAT M358R or AAT M358R(X) with Pka/FXIa were modeled separately using PyMOL Molecular Graphics System 2.5 (https://pymol.org/2/) and ClusPro 2.0 (https://cluspro.bu.edu/login.php), as previously described [17, 23]. Protein Data Base

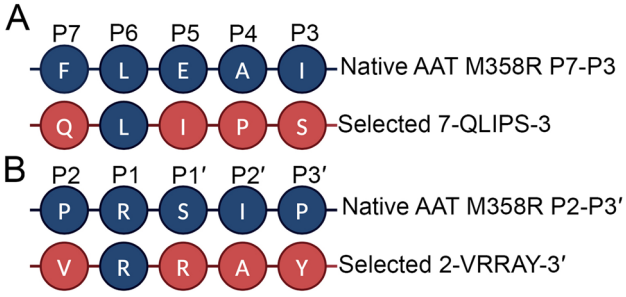

Fig. 1 Schematic representation of the native AAT M358R and selected AAT M358R variants at positions P7-P3′. Native AAT M358R P7-P3 compared to (**A**) selected AAT M358R P7-P3 and (**B**) selected AAT M358R P2-P3′ obtained through phage display

(PDB) files 1OPH, 2ANY, and 1ZJD were used, for AAT M358R, the Pka catalytic domain, and the FXIa catalytic domain, respectively. The distance between the alpha carbon of M358R in AAT M358R or AAT M358R variants and the hydroxyl side group of S195 in Pka/FXIa was determined in each case [10, 30, 46]. Rendered figures were also made using PyMOL.

Statistical analysis and significance testing

Data are presented as the mean ± the standard deviation (SD). Statistical analysis was conducted using GraphPad Prism version 10 (GraphPad Software, Boston, MA, USA). A p-value of <0.05 was taken to be indicative of statistical significance, with AAT M358R serving as the comparator. For multiple comparisons, data were assessed using Brown and Forsythe and Welch one-way ANOVA with Dunnett's T3 post-tests, which is a parametric approach assuming Gaussian distribution of data but not equivalence of standard deviations.

Results

Phage display of AAT M358R P7-P3′ and characterization of 7-QLIPS-3 and 2-VRRAY-3′

We conducted two phage display screens to identify AAT M358R RCL sequences that were the most enriched by biopanning with Pka. To generate libraries amenable to productive phage display probing, no more than five RCL codons were randomized at a time [2, 41]. Two phage display experiments were carried out, spanning from P7-P3 (wild-type AAT sequence FLEAI) and P2-P3′ (AAT M358R sequence PRSIP). After five rounds of biopanning with Pka, the most abundant P7-P3 motif was identified as QLIPS, while the most abundant P2-P3′ motif was identified as VRRAY. The corresponding soluble purified recombinant proteins were named for the motif being probed, with P-numbering identified, as 7-QLIPS-3 and 2-VRRAY-3′ (Fig. 1).

These proteins were characterized by measuring k_2 and SI. Table 1 presents a summary of the kinetic parameters of AAT M358R, 7-QLIPS-3, and 2-VRRAY-3′ with Pka and FXIa. The recombinant protein bearing the motif from P7-P3 phage display, 7-QLIPS-3, inhibited Pka faster than AAT M358R, by 2.2-fold ($p<0.0001$) without significant change to the SI. In contrast to the results with Pka, the protease used for positive selection, 7-QLIPS-3 was significantly slower in inhibiting FXIa, as evidenced by a 3.1-fold reduction in k_2, and was also a less efficient inhibitor, as indicated by its greatly elevated SI, 32.8-fold higher than that of AAT M358R for FXIa. Selectivity for Pka over FXIa was increased 9.2-fold for 7-QLIPS-3 over AAT M358R.

In contrast, the recombinant protein bearing the motif from P2-P3′ phage display, 2-VRRAY-3′, was a significantly less rapid inhibitor of Pka than AAT M358R, on average by 2.1-fold (Table 1). Nevertheless, its selectivity was increased 10.6-fold, on average, due to its greater loss of anti-FXIa activity (23.2-fold) than anti-Pka activity. The efficiency of Pka inhibition by 2-VRRAY-3′ was diminished with respect to AAT M358R, as evidenced by its 2.2-fold increase in SI.

The reactions of AAT M358R, 7-QLIPS-3, and 2-VRRAY-3′ with Pka and FXIa were next examined separately using electrophoresis (Fig. 2). Purified AAT M358R and purified 7-QLIPS-3 migrated as single polypeptide bands of ~45 kDa. When reacted in molar excess with either Pka or FXIa, a portion of these recombinant AAT proteins was converted into covalent AAT-protease complexes of 75–80 kDa, with concomitant disappearance of the catalytic light chains of the proteases from the gel profile. No differences were noted in reaction profiles of AAT M358R or 7-QLIPS-3 with Pka, while with FXIa, 7-QLIPS-3 exhibited a more rapidly migrating polypeptide band of ~41 kDa likely representing 7-QLIPS-3 cleaved at R358-S359, consistent with the

Table 1 Kinetic characterization of protease inhibition by AAT M358R, 7-QLIPS-3, and 2-VRRAY-3′

Name	Second order rate constant (k_2) versus Pka (x10^5 $M^{-1}s^{-1}$)	Second order rate constant (k_2) versus FXIa (x10^5 $M^{-1}s^{-1}$)	Selectivity (Pka k_2: FXIa k_2)	Stoichiometry of inhibition (SI) for Pka	Stoichiometry of inhibition (SI) for FXIa
AAT M358R	0.394 ± 0.019	2.18 ± 0.084	0.181	3.21 ± 0.10	3.47 ± 0.36
7-QLIPS-3	0.870 ± 0.077 ****	0.696 ± 0.049 ****	1.25	2.92 ± 0.42	113 ± 2.7 ****
2-VRRAY-3′	0.180 ± 0.012 ****	0.0940 ± 0.0055 ****	1.91	7.14 ± 0.42 ***	10.4 ± 1.1 ****

Results are the mean of 5 determinations, ± SD. ***, p<0.001****, p <0.0001 versus AAT M358R

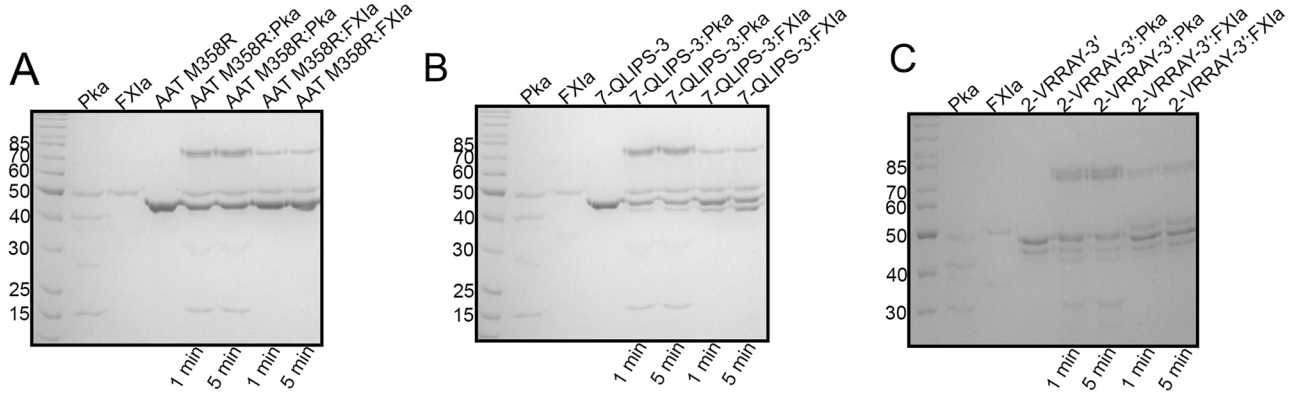

Fig. 2 Electrophoretic profile of reactions of AAT M358R, *7-QLIPS-3, and 2-VRRAY-3′ with Pka or FXIa.* Reactions of 2μM (**A**) AAT M358R, (**B**) 7-QLIPS-3, or (**C**), 2-VRRAY-3′ with Pka (1μM) or FXIa (0.2 μM), for 1–5 min

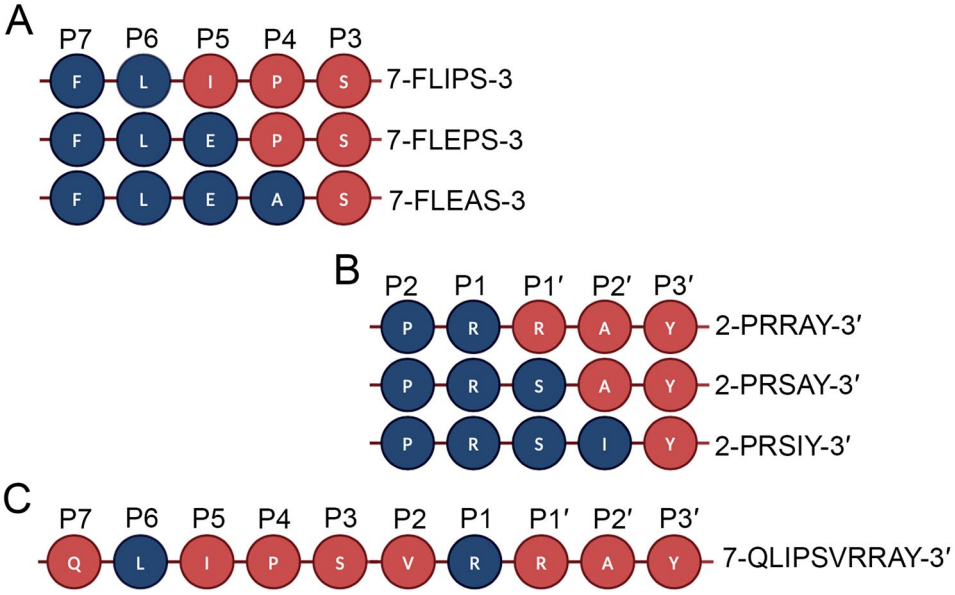

Fig. 3 Schematic diagrams of reversion mutations and combination of selective AAT M358R mutants. Reversion of (**A**) phage-selected 7-QLIPS-3 to original AAT M358R, (**B**) phage-selected 2-VRRAY-3′ to original AAT M358R, and (**C**) the combination of 7-QLIPS-3 and 2-VRRAY-3′ (7-QLIPSVRRAY-3′)

elevated SI of 7-QLIPS-3 for FXIa inhibition (Table 1). In contrast, 2-VRRAY-3′ was heterogeneous, comprising a major full-length ~45 kDa polypeptide and a minor small polypeptide of ~41 kDa. While it formed similar high molecular weight complexes with Pka and FXIa, these were also more heterogeneous than AAT M358R-protease complexes.

Characterization of revertants and combinatorial mutagenesis of selected variants

The mutational strategy involved starting with 7-QLIPS-3 and 2-VRRAY-3′, each containing four unique amino acid substitutions between P7-P3′, compared to AAT M358R, and systematically reversing the mutations, one at a time, back toward the AAT M358R sequence. This generated a total of 6 revertant variants from 7-QLIPS-3 and 2-VRRAY-3′: 7-FLIPS-3, 7-FLEPS-3, 7-FLEAS-3, 2-PRRAY-3′, 2-PRSAY-3′, and 2-PRSIY-3′ (Fig. 3A and B). In addition, the combined variant 7-QLIPSVRRAY-3′ was also expressed (Fig. 3C).

Table 2 summarizes the kinetic activity of AAT M358R, 7-FLIPS-3, 7-FLEPS-3, 7-FLEAS-3, 2-PRRAY-3′, 2-PRSAY-3′, 2-PRSIY-3′, and 7-QLIPSVRRAY-3′ with Pka and FXIa for both k2 and SI. Revertants of 7-QLIPS-3 were without exception found to be more rapid inhibitors of Pka and FXIa than revertants of 2-VRRAY-3′. Their average k_2 values for.

Pka inhibition were between 1.6-fold and 4.5-fold greater than that of AAT M358R. In contrast revertants of 2-VRRAY-3′ on average only exhibited 9.6–18.3% of the k_2 value of AAT M358R for Pka inhibition. Selectivity for Pka was somewhat more favourable due to even greater losses in anti-FXIa activity, with all revertants found to have enhanced selectivity for Pka over FXIa,

Table 2 Kinetic characterization of back mutants and combinatorial mutagenesis

Name	Second order rate constant (k_2) versus Pka (x10^5 $M^{-1}s^{-1}$)	Second order rate constant (k_2) versus FXIa (x10^5 $M^{-1}s^{-1}$)	Selectivity (Pka k_2: FXIa $k_{2)}$	Stoichiometry of inhibition (SI) for Pka	Stoichiometry of inhibition (SI) for FXIa
AAT M358R	0.394 ± 0.019	2.18 ± 0.084	0.181	3.18 ± 0.10	3.48 ± 0.36
7-FLIPS-3	0.620 ± 0.035 ***	0.244 ± 0.011 ****	2.54	5.78 ± 0.31****	185 ± 9.2****
7-FLEPS-3	1.76 ± 0.13 ***	1.06 ± 0.14 ****	1.66	3.18 ± 0.085	87.7 ± 1.0****
7-FLEAS-3	1.33 ± 0.081 ****	3.24 ± 0.18 ***	0.410	1.79 ± 0.035****	1.49 ± 0.028**
2-PRRAY-3′	0.0400 ± 0.0071 ****	0.020 ± 0.01 ****	2.00	19.9 ± 2.4***	28.8 ± 8.2**
2-PRSAY-3′	0.0380 ± 0.0045 ****	0.060 ± 0.01 ****	0.633	16.9 ± 1.9***	14.2 ± 0.84****
2-PRSIY-3′	0.0720 ± 0.0045 ****	0.096 ± 0.006 ****	0.750	11.2 ± 0.54****	9.44 ± 0.24****
7-QLIPSVRRAY-3′	0.164 ± 0.0055 ****	ND	ND	10.7 ± 0.14****	3110 ± 290****

Results are the mean of 5 determinations, ± SD. **, p<0.01, ***, p<0.001, ****, p <0.0001 versus AAT M358R

ranging from 0.66 to 2.00 compared to 0.18 for AAT M358R. This increase in selectivity was offset not only by the decreased rate of inhibition but also by decreased efficiency, as indicated by increased mean SI values ranging from 5.7 to 19.9 (versus 3.18 for AAT M358R).

All three 7-QLIPS-3 revertants exhibited increased rates of Pka inhibition, coupled in two cases (7-FLIPS-3 and 7-FLEPS-3) with decreases in the rate of FXIa inhibition (of 8.9- and 2.1-fold, respectively). 7-FLEAS-3 was the only revertant in which the rate of FXIa inhibition was increased relative to AT M358R, by ~ 1.5-fold. While the SI for Pka inhibition increased 3.8-fold for 7-FLIPS, 7-FLEPS-3 showed no change in SI. Both 7-FLIPS-3 and 7-FLEPS-3 were inefficient inhibitors of FXIa, as judged by substantial increases in SI for FXIa inhibition of 53.2- and 25.2-fold, respectively.

Combining the two motifs in 7-QLIPSVRRAY-3′ resulted in a 2.4-fold decrease in Pka inhibition and abolished detectable k_2 determination of anti-FXIa activity. Furthermore, the SI of 7-QLIPSVRRAY-3′ for Pka and FXIa inhibition increased by 3.36- and 894-fold, respectively. For these reasons the combined variant was not further modified or investigated.

The reactions of all revertant proteins and the double motif combination variant were next examined separately using electrophoresis (Fig. 4). In general, the electrophoretic profiles were consistent with the kinetic analysis. All six revertants formed SDS-stable complexes with both Pka and FXIa, as observed with AAT M358R, 7-QLIPS-3, and 2-VRRAY-3′, with or without the appearance of the ~ 41 kDa cleaved AAT polypeptide, depending on the conditions selected for the 1- or 5-minute reactions (Fig. 4A and F). In contrast, 7-QLIPSVRRAY-3′ showed little or no complex formation with FXIa, and greater cleaved AAT with either Pka or FXIa than any of the revertant proteins, consistent with the remarkably elevated SI values measured for this double motif combination (Fig. 4G).

Additional insights into 7-QLIPS-3 and 7-FLIPS-3 were sought using 7-FLIAI-3 (Supplementary Tables 1 and Supplementary Fig. 1) but it was found to be heterogenous after purification. The variant formed covalent complexes with Pka and FXIa (Supplementary Fig. 1). Estimates of its kinetic parameters were obtained (Supplementary Table 1) but they must be treated with caution given the heterogeneity and the unknown consequences of the contaminating proteins. At face value, a significant but minor contribution of the E362I mutation in 7-QLIPS-3 and 7-FLIPS-3 to enhanced selectivity for Pka (2.6-fold, on average) at the cost of a similar decrease in the rate of Pka inhibition was observed.

AAT M358R, 7-QLIPS-3, 7-FLEPS-3, and 7-QLIPSVRRAY-3′ all exhibited anticoagulant activity in plasma, as indicated by all variants mediating a significant prolongation of the diluted APTT. AAT M358R prolonged clotting the most, followed by 7-QLIPS-3 and 7-FLEPS, which had equivalent activity, followed by 7-QLIPSVRRAY-3′ (Supplementary Fig. 2).

Molecular modeling suggests correlation between the distance and activity

We sought molecular explanations for the selectivity of AAT M358R variants for Pka/FXIa. Utilizing the ClusPro 2.0 web server, we docked modeled AAT M358R variants to modeled protease catalytic domains and selected the lowest free energy version of ten modeled encounter complexes to gain insights into potential molecular explanations. Table 3 delineates the distances (in angstroms, Å) between the alpha carbon of M358R in AAT M358R variants and the hydroxyl side chain of S195 in Pka/FXIa, as one potential measure of the ease or difficulty of proceeding along the reaction pathway following formation of an initial complex between these protein reactants.

The modeled distance between the catalytic domain of Pka S195, and the reactive bond of R358 in AAT M358R, was 11.5Å. Conversely, the modeled distance between the catalytic domain of FXIa and S195, and the reactive bond of R358 in AAT M358R, was 3.3Å. For 7-QLIPS-3 and the revertants representing faster reactions for Pka

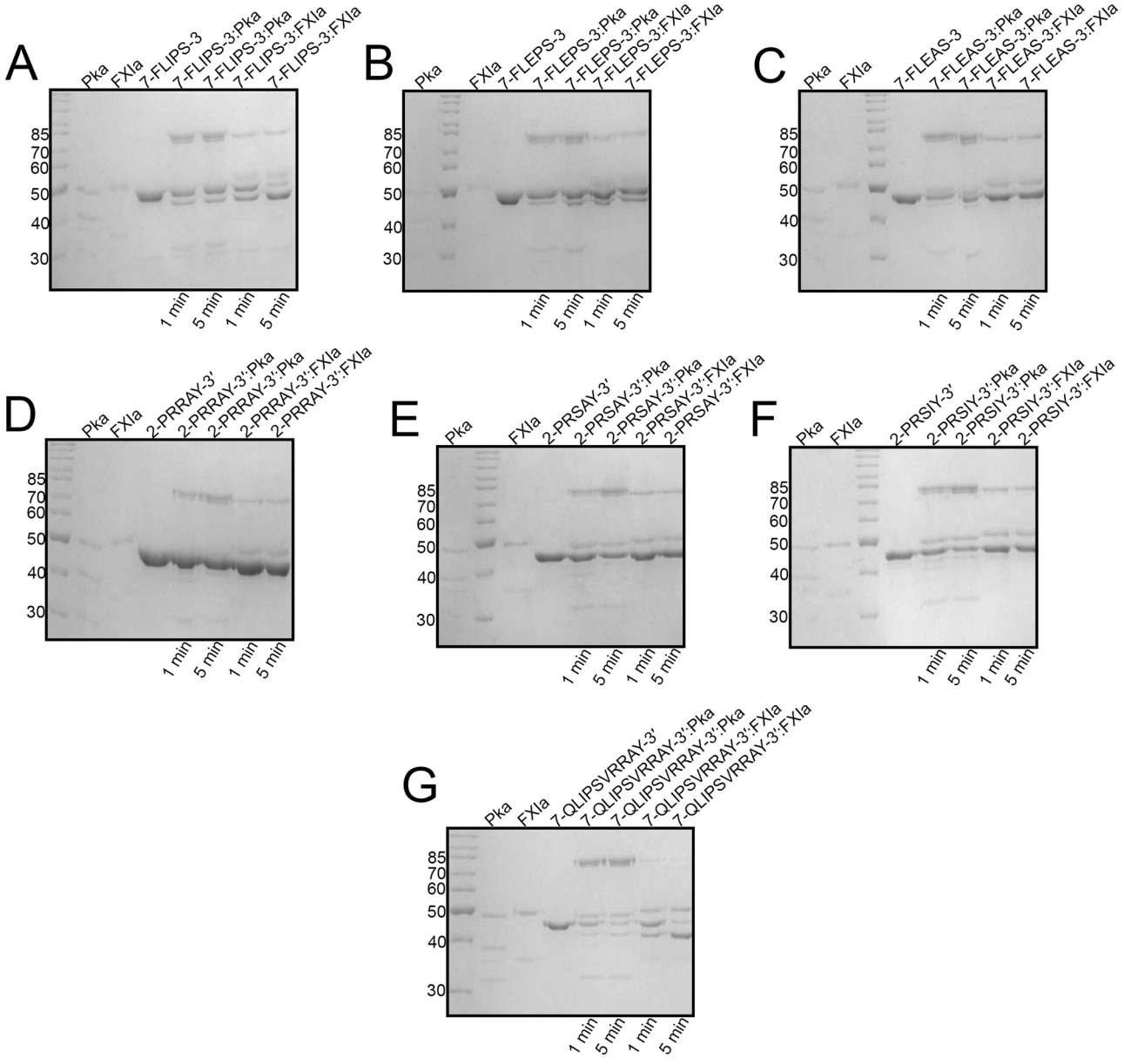

Fig. 4 Electrophoretic profile of reactions of revertants and combination variant with Pka and FXIa. Reaction of (2μM) AAT variants (identified above the stained gel images) with Pka (1μM) or FXIa (0.2 μM) for times specified below each panel

and slower reactions for FXIa, shorter distances between RCL and Pka, and longer distances between RCL and FXIa, were observed. For instance, there was a reduction of 71.3% in this distance between 7-FLEPS-3 and Pka, while an increase of 8.3% was noted between 7-FLEPS-3 and FXIa. Conversely, for 2-VRRAY-3' and the revertants representing slower reactions for both Pka and FXIa, longer distances between RCL and Pka/FXIa were modeled; between 2-PRRAY-3′ and Pka, this distance increased by 135.6%, and by 1230% between 2-PRRAY-3′ and FXIa.

Figure 5 represents a close-up model of the initial, non-covalent encounter complex of the light chain catalytic domain of Pka/FXIa (cyan/purple) docked to AAT M358R or 7-FLEPS-3 or 2-PRRAY-3' RCL (green, orange for changed residues). This figure provides visual insight into the differences among the initial, optimal, and least favorable interactions for the three selected mutants.

Discussion

The current study sought to replicate the success of a previous strategy of biopanning phage-displayed hypervariable AAT libraries with a bait protease, combinatorial mutagenesis, and partial reversion of mutant sequences toward the wild-type, substituting Pka for FXIa [3] Our previous work using FXIa identified AAT-RC-2, a form of AAT M358R with three additional mutations (P7-P3′

Table 3 Modeled distances between alpha carbon of R358 and S195 hydroxyl side chain in AAT M358R and variant encounter complexes

Name of inhibitor protein	Pka distance (Å)	FXIa distance (Å)
AAT M358R	11.5	3.3
7-QLIPS-3	4.4	4.9
7-FLIPS-3	6.3	8.7
7-FLEPS-3	3.3	3.6
7-FLEAS-3	3.4	3.1
2-VRRAY-3′	12.8	18.2
2-PRRAY-3′	27.1	43.9
2-PRSAY-3′	27.0	23.9
2-PRSIY-3′	23.4	15.0
7-QLIPSVRRAY-3′	15.6	54.9

FLEA**EP**R**STE**, substitutions bolded) as being 25-fold more selective for FXIa over Pka than AAT M358R, and 470-fold more selective for FXIa over thrombin than AAT M358R [17]. AAT RC-2 was the most FXIa-specific inhibitor of a set of four candidate proteins comprising two motifs selected by phage or bacterial display (AAT-RC) and stepwise revertants (AAT RC-1, 2, and – 3) that changed the AAT RC RCL sequence back towards AAT M358R one residue at a time. AAT-RC-2's increased selectivity towards FXIa was achieved with a 31% increase in its rate of FXIa inhibition and no increase in SI for FXIa compared to those kinetic parameters of AAT M358R [17]. In the current study, the analogous optimal variant was 7-FLEPS-3, a revertant of the phage

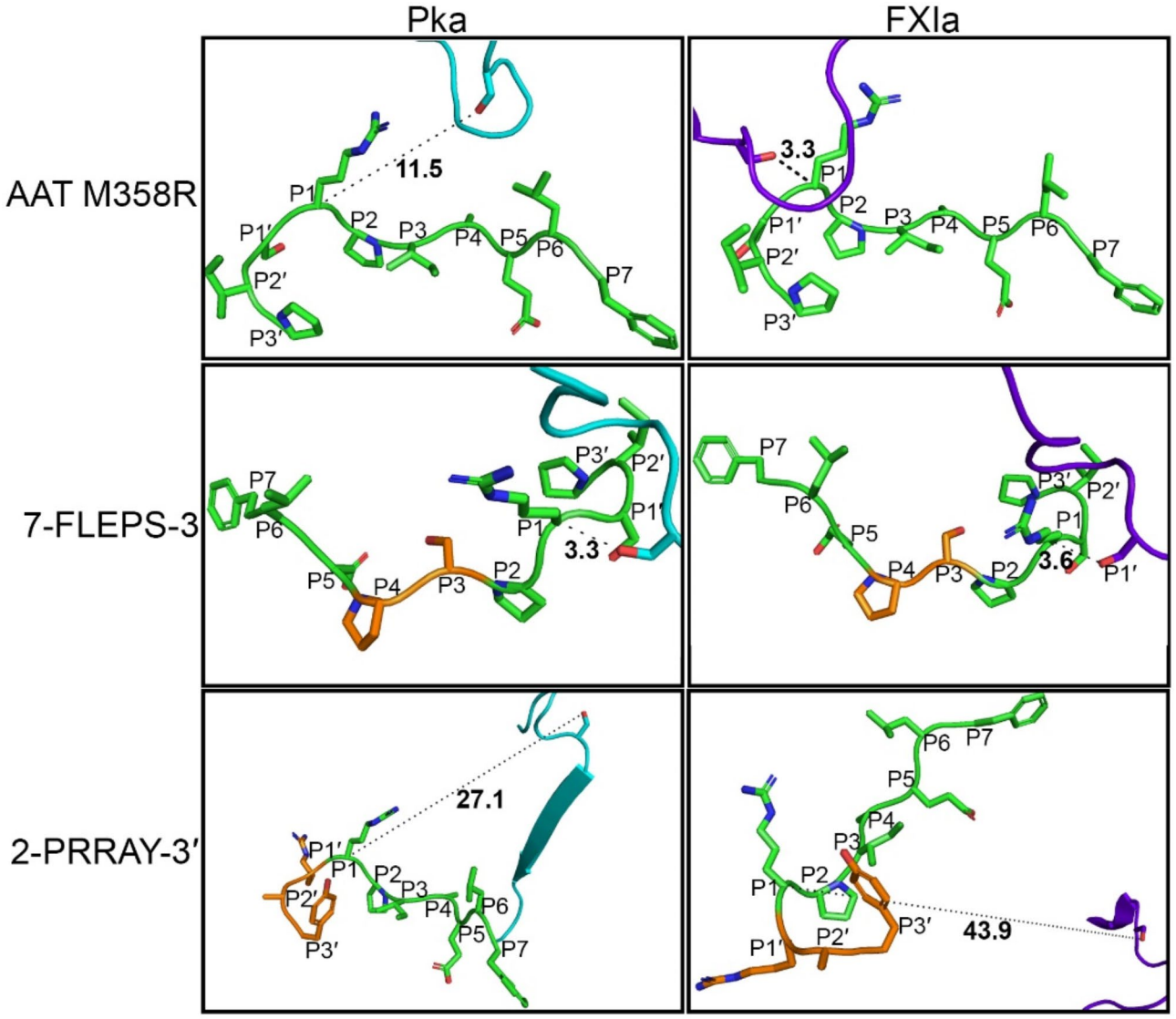

Fig. 5 Molecular models of Pka and FXIa encounter complex to AAT M358R variants. Crystal structures of the catalytic domain of Pka (cyan, PDB 2ANY) or catalytic domain of FXIa (purple, PDB 1ZJD), and AAT M358R (original sequence in green; variants in orange, PDB 1OPH) were docked using ClusPro 2.0 as described in Methods. Yellow dashed lines indicate distance (Å) predicted between the alpha carbon of R358 in AAT M358R variants and the hydroxyl side chain of S195 in Pka/FXIa

display-selected motif 7-QLIPS-3. 7-FLEPS-3 was 9.2-fold more selective for Pka over FXIa than AAT M358R, a gain in selectivity achieved with a concomitant 4.5-fold increase in the rate of Pka inhibition and no significant increase in SI. In contrast to our previous studies, no gain in selectivity was achieved by combining the RCL motifs identified by separate biopanning campaigns in 7-QLIPSVRRAY-3′, although the possibility that stepwise reversion of the combined motif towards the AAT M358R might have yielded gains in selectivity cannot be excluded.

RCL motifs identified using T7 phage display of AAT are subject to several uncertainties. They may behave differently with respect to their interaction with proteases when expressed in the molecular context of a stand-alone soluble protein than when expressed as a coat protein-serpin fusion protein on the bacteriophage surface [6]. Although we formally demonstrated that AAT M358R fused to T7 bacteriophage coat protein 10 formed a covalent complex with thrombin [41] this may not be the case with other bait proteases, for which a high affinity non-covalent encounter complex may be sufficient for selection. Moreover, because the screened library is hypervariable, not all mutations in the selected motif may contribute to enhanced interactions with the bait protease, and stepwise reversion may reveal variants with superior properties than the full selected motif.

The QLIPS motif yielded a more active Pka inhibitor than the VRRAY motif when expressed as soluble AAT M358R proteins 7-QLIPS-3 and 2-VRRAY-3′. Reverting 7-QLIPS-3 to 7-FLIPS-3 yielded higher selectivity for Pka at the cost of increased SI. While the SI is theoretically 1, reflecting perfect 1:1 covalent complex inhibition of a target protease, recombinant engineered serpins frequently display higher SI values, for instance due to a branched pathway yielding both covalent serpin-inhibitory complex and cleaved serpin products [14]. Reverting 7-FLIPS-3 to 7-FLEPS-3 produced the most selective Pka inhibitor of the P7-P3′ mutants, without increasing SI. Finally, reverting 7-FLEPS-3 to 7-FLEAS-3 enhanced FXIa inhibition more than Pka inhibition, eliminating most of the gains in selectivity achieved with 7-FLEPS-3. This comparison identifies the P4 mutation A355P as being the most important contributor to the increased Pka selectivity of 7-QLIPS-3, 7-FLIPS-3, and 7-FLEPS-3. This mutation has not previously been described in the literature, either in mutagenesis studies [39] or in patients with AAT deficiency [44]. Pigment epithelium-derived factor (PEDF) is the only serpin known to contain a proline at P4, and it is non-inhibitory [35]. Proline residues are helix-breaking, and the increased peptide rigidity they elicit could lock the 7-FLEPS-3 RCL into a favourable conformation for interacting with Pka, especially in combination with Pro357 at P2. 7-FLEPS-3 was the most selective variant tested whose selectivity was not gained at the cost of increased SI. Increased SI is undesirable given that it indicates not only reduced efficiency as an inhibitor, due to cleavage rather than complexation, but also the possibility of promoting inflammation, given that cleaved AAT has been shown to be pro-inflammatory in cell culture [28].

Our results overlap with some previous studies of wild-type AAT. Previously Phe352 was mutated to Glu in the wild-type AAT background without decreasing its rate of elastase inhibition, consistent with our finding that F352Q in the 7-QLIPS-3 (AAT M358R) context was functional. Mutations to the P5 Glu residue in wild-type AAT were also previously shown to increase the SI by ~4-fold [5], consistent with our findings that restoration of P5 Glu in 7-FLEPS-3 reduced the SI relative to 7-FLIPS-3, although the similar SI of 7-QLIPS-3 argues for cooperativity between residues in that context. RCL cooperativity has been noted in previous mutagenic studies of AAT [19].

The VRRAY motif selected via biopanning of the second phage display library was not as effective as the QLIPS motif when recreated in soluble recombinant 2-VRRAY-3′. While this variant formed covalent complexes with Pka and FXIa and inhibited the proteases at measurable rates, its rate of inhibition of Pka was 2.5-fold lower than AAT M358R and its increased selectivity was achieved at the cost of an elevated SI. There are no natural serpins with a natural Arg-Arg reactive centre. AAT variants with P2-P1′ sequences of RRS, PRR, and RRC were found to be more efficient inhibitors of Activated Protein C than a KRK variant [36] Reversion of 2-VRRAY-3′ to PRRAY-3′ further reduced the rate of inhibition of Pka, and SI values were elevated for all VRRAY-related variants, including 2-PRSIY-3′, which is a single residue mutant (P361Y). Given the preference of Pka for cleaving substrates C-terminal to Arg residues [4, 13, 53], it is possible that the observed SI elevation could have arisen from Pka cleavage at either P1-P1′ or P1′-P2′, with the latter leading to substrate rather than inhibitor behaviour of 2-VRRAY-3′. This feature may have led to enhanced recognition in biopanning of phage exhibiting this motif that was not reproduced when transferred to soluble serpin form. Alternatively, the VRRAY-bearing phage may have harboured an unforeseen growth advantage that along with their reactivity with Pka promoted their abundance in the Pka-selected pool.

Our approach was to alter AAT to make it a specific inhibitor of Pka, like other therapeutic agents used to treat or control HAE or envisioned for such use. Others have sought to make AAT simultaneously able to inhibit Pka, FXIIa, and FXIa, and not other proteases, reasoning that such an engineered protein could have multiple clinical uses in disorders related to thromboinflammation [8]

The AAT variant with the most potent inhibition of the three target proteases, SLLR/V (P4-P1′), perhaps unsurprisingly, has no overlap to the QLIPS or VRRAY series of variants described in this study. The 7-FLEAS-3 variant, intriguingly, inhibited both Pka and FXIa with rate constants higher than AAT M358R, in both cases, and could be considered as a candidate for control of thromboinflammation. A consideration for all mutagenesis studies is that the more modifications are introduced into a human protein, the greater the likelihood of eliciting an immune response in patients; 7-FLEAS-3 has only two variant residues compared to five in SLLR/V.

We found that the overall fitness of our variant AAT molecules as Pka inhibitors correlated reasonably well with the ClusPro 2.0-modeled distance to the active site S195 of Pka, suggesting that we had selected for effective encounter complex formation. In the serpin mechanism, nucleophilic attack by the active site serine of the protease on the carbonyl carbon of the serpin P1 residue in the P1-P1′ peptide bond is an essential step in the progression from encounter complex to tetrahedral intermediate to acyl intermediate to stable serpin-enzyme complex [20]. We assumed that a modeled complex in which the protease hydroxyl group of the protease serine residue was closer to its reactive centre target in an AAT variant would predict faster inhibition rates than for a variant in which this distance was greater. Our assumption was supported by the measured distances, because variants with shorter distances than in AAT M358R between the key reactive groups were faster inhibitors of the modeled protease than AAT M358R and those with longer distances inhibited the modeled protease less rapidly. However, the modeled distance between the groups in AAT M358R, for Pka, was a substantial 11.5 Å, which indicates that energy-minimized ClusPro 2.0 modeling provides only an early model of a reversible encounter complex, one which must evolve to bring the reactant groups into closer proximity. While compatibility between RCL residues and protease active sites would seem a more critical parameter in assessing encounter complex fitness than the distance on which we focused, our modeling did not identify electrostatic or hydrophobic interactions between these residues that were strengthened by accelerator variants, unlike in our previous use of ClusPro 2.0 to rationalize AAT M35R variant interactions with FXIa. The latter approach identified the facilitation of hydrogen bonds to K192 in FXIa as correlating with enhanced rates of FXI inhibition [17]. Thus, the modeled distances serve only as a rough guide to variant fitness as an inhibitor, especially for distances of 20 Å or more.

Altering serpin specificity via protein engineering is a task with multiple molecular hurdles. The engineered serpin must form an encounter complex with the target protease efficiently, ideally by engaging the active site without clashes, and its reactive centre must be efficiently cleaved. The engineered RCL must then integrate into the underlying β sheet of the serpin rapidly; failure to do so will allow escape of the trapped protease. Incompatibilities in the last step can underlie SI elevation [17]. Modelling the fitness of the variant inhibitor for SI elevation would require advanced molecular dynamics modelling beyond the scope of this study and the capabilities of our laboratory.

Others have used structural modeling a priori to design AAT mutagenesis [34], or a combination of cleavage preference information and functional testing of a protein library to change AAT specificity [8, 36]. All strategies have yielded novel variants with desired or more optimal properties for the biotechnological problem at hand; it is therefore not possible to endorse one method over another as being more efficient or successful.

Conclusion

Purified C1INH products are currently used to prevent or treat HAE, despite C1INH's relatively slow rate of Pka inhibition of $\sim 2.6 \times 10^4$ $M^{-1}s^{-1}$ [21, 52]. Our results in this study suggest that 7-FLEPS-3, an AAT M358R variant with two additional substitutions, is a candidate for further testing in animal models of HAE, given its 7-fold faster rate of Pka inhibition. Further, while we found that phage display and subsequent refinement of variant sequences by reversion mutagenesis were successful in identifying this promising variant, combining different RCL motifs identified in separate parts of the RCL was more effective when FXIa was the target than when Pka was employed [17].

Abbreviations

AAT	Alpha-1 Antitrypsin
AAT M358R	Alpha-1 Antitrypsin M358R
APC	Activated protein C
7-FLEAS-3	Alpha-1 Antitrypsin I356S, M358R
7-FLEPS-3	Alpha-1 Antitrypsin A355P, I356S, M358R
7-FLIAI-3	Alpha-1 Antitrypsin E354I, M358R
7-FLIPS-3	Alpha-1 Antitrypsin E354I, A355P, I356S, M358R
2-PRRAY-3	Alpha-1 Antitrypsin M358R, S359R, I360A, P361Y
2-PRSAY-3	Alpha-1 Antitrypsin M358R, I360A, P361Y
2-PRSIY-3	Alpha-1 Antitrypsin M358R, P361Y
7-QLIPS-3	Alpha-1 Antitrypsin F352Q, E354I, A355P, I356S, M358R
7-QLIPSVRRAY-3 ′	Alpha-1 Antitrypsin F352Q, E354I, A355P, I356S, P357V, M358R, S359R, I360A, P361Y
2-VRRAY-3 ′	Alpha-1 Antitrypsin P357V, M358R, S359R, I360A, P361Y
C1INH	C1-inhibitor
Coomassie Brilliant Blue	0.1% Coomassie R-250 in 40% ethanol and 10% acetic acid
Destain	10% acetic acid and 50% methanol
E. coli	Escherichia coli
FXIa	Activated Factor XI
FXIIa	Activated Factor XII
h	Hour
HAE	Hereditary Angioedema
IPTG	Isopropyl β-D-1-thiogalactopyranoside
k2	Second-order rate constant

kDa	Kilodalton
LB	Luria broth
LB-amp	Luria broth with ampicillin
M9LB	M9 salts in Luria broth
M	Molar
M− 1s− 1	Moles per liter per second
mM	Millimolar
min	Minute
mg	Milligram
µg	Microgram
µl	Microliter
µM	Micromolar
ml	Milliliter
nM	Nanomolar
PBS	Phosphate buffered saline
PEDF	Pigment epithelium-derived factor
pfu	Plaque forming units
PPNE Buffer	20mM sodium phosphate (pH 7.4), 0.1% (w/v) polyethylene glycol 8000, 100mM sodium chloride, and 0.1mM disodium ethylenediaminetetraacetic acid
Pka	Plasma kallikrein (KLKB1)
RCL	Reactive center loop
rpm	Revolutions per minute
RR	Arginine-Arginine
s	Second
S-2302	Chromogenic substrate for activated plasma kallikrein
S-2366	Chromogenic substrate for activated Factor XI
SD	Standard deviation
SDS	Sodium dodecyl sulphate
SDS Buffer	0.2 M Tris-HCl (pH 6.8), 0.4 M DTT, 277mM SDS, 6mM bromophenol blue, and 4.3 M glycerol
SI	Stoichiometry of inhibition
v/v	Volume/volume
w/v	Weight/volume
Å	Angstrom
°C	Degree in Celsius
%	Percentage
±	Plus or minus

Supplementary Information

The online version contains supplementary material available at https://doi.org/10.1186/s12896-025-00956-8.

Supplementary Material 1

Supplementary Material 2

Supplementary Material 3

Supplementary Material 4

Supplementary Material 5

Acknowledgements
The authors gratefully acknowledge the expert advice of Dr. Sara Andres, Associate Professor, Department of Biochemistry and Biomedical Sciences, McMaster University, regarding protein structural modeling.

Author contributions
SS conducted phage display of AAT M358R P2-P3', analyzed the inhibitory kinetics of all the variants, conducted all protein structural modeling, and was a major contributor in writing and revising the manuscript. TS conducted phage display of AAT M358R P7-P3 and did preliminary characterization of some variants. NCT expressed revertants and combined forms of the AAT M358R variants. VB provided technical training and oversight to SS, TS, and NCT with their contributions. WPS designed the study, secured competitive research funding, provided overall supervision for all experiments and was a major contributor in writing and revising the manuscript. All authors read and approved the final manuscript.

Funding
Canadian Blood Services Discovery Research Grant DRG-WS2023 award to William P. Sheffield, and Canadian Blood Services Graduate Fellowship Program award to Sangavi Sivananthan.

Data availability
All data generated or analyzed during this study are included in this published article and its supplementary information (additional) files.

Declarations

Ethics approval and consent to participate
Not applicable.

Consent for publication
Not applicable.

Competing interests
The authors declare no competing interests.

Received: 7 October 2024 / Accepted: 7 March 2025
Published online: 12 March 2025

References

1. Banerji A, et al. Long-term prevention of hereditary angioedema attacks with lanadelumab: the HELP OLE study. Allergy. 2022;77(3):979–90.
2. Bhakta V, Gierczak RF, Sheffield WP. Expression screening of bacterial libraries of Recombinant alpha-1 proteinase inhibitor variants for candidates with thrombin inhibitory capacity. J Biotechnol. 2013;168(4):373–81.
3. Bhakta V, et al. Identification of an alpha-1 antitrypsin variant with enhanced specificity for factor XIa by phage display, bacterial expression, and combinatorial mutagenesis. Sci Rep. 2021;11(1):5565.
4. Capraro J, et al. Proteolytic cleavage at twin arginine residues affects structural and functional transitions of lupin seed 11S storage Globulin. PLoS ONE. 2015;10(2):e0117406.
5. Chaillan-Huntington CE. and P. A. Patston influence of the P5 residue on alpha1-proteinase inhibitor mechanism. J Biol Chem. 1998;273(8):4569–73.
6. Danner S, Belasco JG. T7 phage display: a novel genetic selection system for cloning RNA-binding proteins from cDNA libraries. Proc Natl Acad Sci U S A. 2001;98(23):12954–9.
7. Davis AE. 3rd C1 inhibitor and hereditary angioneurotic edema. Annu Rev Immunol. 1988;6:595–628.
8. de Maat S, et al. Design and characterization of alpha1-antitrypsin variants for treatment of contact system-driven thromboinflammation. Blood. 2019;134(19):1658–69.
9. de Souza L, R, et al. Serpin phage display: the use of a T7 system to probe reactive center loop libraries with different Serine proteinases. Methods Mol Biol. 2018;1826:41–64.
10. Dementiev A et al. Canonical inhibitor-like interactions explain reactivity of alpha1-proteinase inhibitor Pittsburgh and antithrombin with proteinases. J Biol Chem. 2003;278(39):37881–7.
11. Deng X, et al. Advances in the T7 phage display system (Review). Mol Med Rep. 2018;17(1):714–20.
12. Donaldson VH. and R. R. Evans. A Biochemical Abnormality in Herediatry Angioneurotic Edema: Absence of Serum Inhibitor of C' 1-Esterase. Am J Med. 1963;35:37–44.
13. Duckert P, Brunak S. and N. Blom prediction of proprotein convertase cleavage sites. Protein Eng Des Sel. 2004;17(1):107–12.
14. Gettins PG. Serpin structure, mechanism, and function. Chem Rev. 2002;102(12):4751–804.
15. Gigli I, et al. Interaction of plasma Kallikrein with the C1 inhibitor. J Immunol. 1970;104(3):574–81.
16. Grover S, et al. C1 inhibitor deficiency enhances contact pathway-mediated activation of coagulation and venous thrombosis. Blood. 2023;141(19):2390–401.
17. Hamada M, et al. Stepwise reversion of multiply mutated Recombinant antitrypsin reveals a selective inhibitor of coagulation factor XIa as active as the M358R variant. Front Cardiovasc Med. 2021;8:647405.

18. Heeb M et al. J. Inhibition of activated protein C by Recombinant alpha 1-antitrypsin variants with substitution of arginine or leucine for methionine358. J Biol Chem. 1990;265 4 2365–9.
19. Hopkins PC, Pike RN, Stone SR. Evolution of Serpin specificity: cooperative interactions in the reactive-site loop sequence of antithrombin specifically restrict the Inhibition of activated protein C. J Mol Evol. 2000;51(5):507–15.
20. Huntington JA. Serpin structure, function and dysfunction. J Thromb Haemost. 2011;9(Suppl 1):26–34.
21. Kajdacsi E et al. Patterns of C1-Inhibitor/Plasma Serine protease complexes in healthy humans and in hereditary angioedema patients. Front Immunol. 2020;11:794.
22. Karnaukhova E. C1-Inhibitor: structure, functional diversity and therapeutic development. Curr Med Chem. 2022;29(3):467–88.
23. Kozakov D, et al. The cluspro web server for protein-protein Docking. Nat Protoc. 2017;12(2):255–78.
24. Landerman NS, et al. Hereditary angioneurotic edema. II. Deficiency of inhibitor for serum Globulin permeability factor and/or plasma Kallikrein. J Allergy. 1962;33:330–41.
25. Lin L, Wu M. and J. Zhao the initiation and effects of plasma contact activation: an overview. Int J Hematol. 2017;105(3):235–43.
26. Markland W, Ley AC. and R. C. Ladner iterative optimization of high-affinity protease inhibitors using phage display. 2. Plasma Kallikrein and thrombin. Biochemistry. 1996;35(24):8058–67.
27. Martello JL, Woytowish MR. and H. Chambers Ecallantide for treatment of acute attacks of hereditary angioedema. Am J Health Syst Pharm. 2012;69(8):651–7.
28. Moraga F, Lindgren S, and S. Janciaskiene. Effects of noninhibitory alpha-1-antitrypsin on primary human monocyte activation in vitro. Arch Biochem Biophys. 2001;386(2):221–6.
29. Motta G, Juliano L. and J. R. Chagas human plasma Kallikrein: roles in coagulation, fibrinolysis, inflammation pathways, and beyond. Front Physiol. 2023;14:1188816.
30. Navaneetham D, et al. Structural and mutational analyses of the molecular interactions between the catalytic domain of factor XIa and the Kunitz protease inhibitor domain of protease nexin 2. J Biol Chem. 2005;280(43):36165–75.
31. Olson ST, Bjork I. and J. D. Shore. kinetic characterization of heparin-catalyzed and uncatalyzed Inhibition of blood coagulation proteinases by antithrombin. Methods Enzymol. 1993;222:525–59.
32. Owen MC et al. Mutation of antitrypsin to antithrombin. Alpha 1-antitrypsin Pittsburgh (358 Met leads to Arg), a fatal bleeding disorder. N Engl J Med. 1983;309(12):694–8.
33. Patston PA, et al. Reactivity of alpha 1-antitrypsin mutants against proteolytic enzymes of the kallikrein-kinin, complement, and fibrinolytic systems. J Biol Chem. 1990;265(18):10786–91.
34. Polderdijk SG et al. Design and characterization of an APC-specific Serpin for the treatment of hemophilia. Blood. 2017;129(1):105–13.
35. Sanrattana W, Maas C. and S. De Maat SERPINs-From trap to treatment. Front Med (Lausanne) 2019;6:25.
36. Sanrattana W et al. A reactive center loop-based prediction platform to enhance the design of therapeutic SERPINs. Proc Natl Acad Sci USA. 2021;118(45).
37. Schapira M, et al. Recombinant alpha 1-antitrypsin Pittsburgh (Met 358---- Arg) is a potent inhibitor of plasma Kallikrein and activated factor XII fragment. J Clin Invest. 1986;77(2):635–7.
38. Schmaier AH. The contact activation and Kallikrein/kinin systems: pathophysiologic and physiologic activities. J Thromb Haemost. 2016;14(1):28–39.
39. Scott BM. and W. P. Sheffield engineering the Serpin alpha(1) -antitrypsin: A diversity of goals and techniques. Protein Sci. 2020;29(4):856–71.
40. Scott CF, et al. Alpha-1-antitrypsin-Pittsburgh. A potent inhibitor of human plasma factor XIa, Kallikrein, and factor XIIf. J Clin Invest. 1986;77(2):631–4.
41. Scott BM, et al. Phage display of the Serpin alpha-1 proteinase inhibitor randomized at consecutive residues in the reactive centre loop and biopanned with or without thrombin. PLoS ONE. 2014;9(1):e84491.
42. Sinnathamby ES, et al. Hereditary angioedema: diagnosis, clinical implications, and pathophysiology. Adv Ther. 2023;40(3):814–27.
43. Stolz LE, Horn PT. Ecallantide: a plasma Kallikrein inhibitor for the treatment of acute attacks of hereditary angioedema. Drugs Today (Barc). 2010;46(8):547–55.
44. Strnad P, McElvaney NG, Lomas DA. Alpha(1)-Antitrypsin deficiency. N Engl J Med. 2020;382(15):1443–55.
45. Syed YY. Lanadelumab: A review in hereditary angioedema. Drugs. 2019;79(16):1777–84.
46. Tang J, et al. Expression, crystallization, and three-dimensional structure of the catalytic domain of human plasma Kallikrein. J Biol Chem. 2005;280(49):41077–89.
47. Travis J, et al. Kinetic studies on the interaction of alpha 1-proteinase inhibitor (Pittsburgh) with trypsin-like Serine proteinases. Biol Chem Hoppe Seyler. 1986;367(9):853–9.
48. Wedi B. Lanadelumab to treat hereditary angioedema. Drugs Today (Barc). 2019;55(7):439–48.
49. Wedner HJ. Hereditary angioedema: pathophysiology (HAE type I, HAE type II, and HAE nC1-INH). Allergy Asthma Proc. 2020;41(Suppl 1):S14–7.
50. Wilkerson RG. and J. J. Moellman hereditary angioedema. Emerg Med Clin North Am. 2022;40(1):99–118.
51. Wu Y. Contact pathway of coagulation and inflammation. Thromb J. 2015;13:17.
52. Wuillemin WA, et al. Modulation of contact system proteases by glycosaminoglycans. Selective enhancement of the Inhibition of factor XIa. J Biol Chem. 1996;271(22):12913–8.
53. Xie Z, et al. Discovery and development of plasma Kallikrein inhibitors for multiple diseases. Eur J Med Chem. 2020;190:112137.
54. Zahedi K, Prada AE, Davis AE. 3rd structure and regulation of the C1 inhibitor gene. Behring Inst Mitt. 1993;(93):115–9.

Publisher's note

Springer Nature remains neutral with regard to jurisdictional claims in published maps and institutional affiliations.